MSc in Photonics

Universitat Politècnica de Catalunya (UPC)
Universitat Autònoma de Barcelona (UAB)
Universitat de Barcelona (UB)
Institut de Ciències Fotòniques (ICFO)

PHOTONICSBCN

http://www.photonicsbcn.eu

Master in Photonics

MASTER THESIS WORK

FERROELECTRIC MATERIALS FOR PHOTOVOLTAICS.

Diego Vázquez Calvo.

**Supervised by Dr. Sandra Bermejo, (UPC)
Pr. Josep Foncuberta (ICMAB)
Dr. Ignasi Fina (ICMAB)**

Presented on date 7th September 2017

Registered at

**Escola Tècnica Superior
d'Enginyeria de Telecomunicació de Barcelona**

Ferroelectric materials for photovoltaic.

Diego Vázquez Calvo

ICMAB, Instituto de Ciencia de Materiales de Barcelona, Campus de la UAB 08193 Bellaterra, Spain.

E-mail: `Vazquezcalvodiego@gmail.com`

August 31, 2017

Abstract.

Ferroelectric photovoltaic has been intensively studied during the last years due to possible high efficient charge separation by presence of an internal electric field. Ferroelectric materials show permanent electrical polarization. Ideally, electric contacts would screen the polarization, but if screening is not perfect, it results in the generation of depolarization field. In this report, we study the photoelectric response of $LuMnO_3$ that shows a small bandgap compared to archetypical ferroelectric materials and a sizeable internal polarization. We have studied its photoresponse dependence on polarization state.

1. Introduction

In the last few decades, a huge investment has been done in solar energy conversion. Photovoltaic is one of the most promising renewable energy technologies to solve the energy crisis that is coming due to the overexploitation of fossil fuels. However further improvements are needed to obtain a higher efficiency and lower fabrication costs to make this technology competitive.

Nowadays, p-n junctions devices based on silicon are the most usual, giving efficiencies around 20% [1,2]. However, the fabrication cost of these devices is high and not competitive. Then a lot of researchers are focused on finding alternative mechanisms that increase the efficiency on materials with a lower fabrication process cost and find a balance. Some of these mechanisms are the use of heterojunctions, thin films technology or ferroelectric materials to maximize the energy conversion[3,4,5].

In conventional solar cells, a p-n junction is used to generate a field that allows separating the charges but this field is concentrated around the interface[6]. This electric field is limited by the material bands. Conversely in ferroelectrics, internal field is inherent to the material and it extends along the whole device enhancing charge separation [4,7].

In semiconductors materials electron-holes pairs (excitons) are generated in a material when an incident photon has an energy above the bandgap energy. An electron

is promoted to the conduction band leaving a hole in the valence band. This electrons-holes pairs generate a photovoltage due to differences in the quasi-Fermi levels and a photocurrent when the charges are collected. Then we can extract power from the material. It is established that materials with a bandgap around $E_g \simeq 1.5eV$ allows maximum energy conversion for solar spectrum.

Ferroelectrics generate low photocurrents principally due to wide bandgaps. Low bandgap ferroelectric materials are promising for photovoltaic applications due to wider solar spectrum can be used to generate excitons. Then we find two different paths to this propose: engineering archetypical FE materials[8] ($BaTiO_3/BiFeO_3$) to obtain a smaller bandgap or find FE materials with an inherent lower bandgap.

Our material under study $LuMnO_3$ is interesting because it is a small bandgap ferroelectric material which shows a bandgap $E_g \simeq 1.5eV$ [9]. $E_g \simeq 1.5eV$ is similar to the ideal limit according to the Shockley and Queisser limit [10]. $LuMnO_3$ also shows a sizeable polarization value $P \simeq 15\mu C/cm^2$. These characteristics make $LuMnO_3$ a promising material in the development of photovoltaic technology.

2. State of the Art.

In this section, I will discuss the exclusive mechanisms that drive photoresponse in ferroelectric materials: depolarization field, bulk photovoltaic effect and domain wall.

2.1. Depolarization Field.

Ferroelectric materials host a permanent polarization state which generates an internal field along the sample named depolarization field. Polarization state is controllable by applying an external bias which reverses it when the bias goes above the coercive field. Then the depolarization field is controllable. This field could be a high efficient mechanism for photocharges separation if it is not totally screened by electrodes, whose carriers cancel the polarization field. Figure 1 shows the screened and not screened configuration. In the Fig a) and d) there is a representation of the device without and with contacts respectively. In the first case, there are not electrodes, then the field is not screened and the sample host a depolarization field. As there is a field along the sample conduction and valence bands tilt as is shown in the Fig b) and c) collecting the generated carriers, like the polarization state is switchable each figure shows each polarization state. In the d), e), f) figures we have different situation, $LuMnO_3$ is sandwiched between two metal electrodes. Metal electrons screen the depolarization field resulting in a null net field. As there is not a field in this case the bands remain flat and there is not an effect of depolarization field in charge separation, and either in the presence of photocurrent.

The free carriers apportioned by the electrodes, to screen the polarization, do not have the same mass centre than the polarization charges giving rise to dipoles in the interface between them [11]. Then these dipoles barrier modifies the effective injection
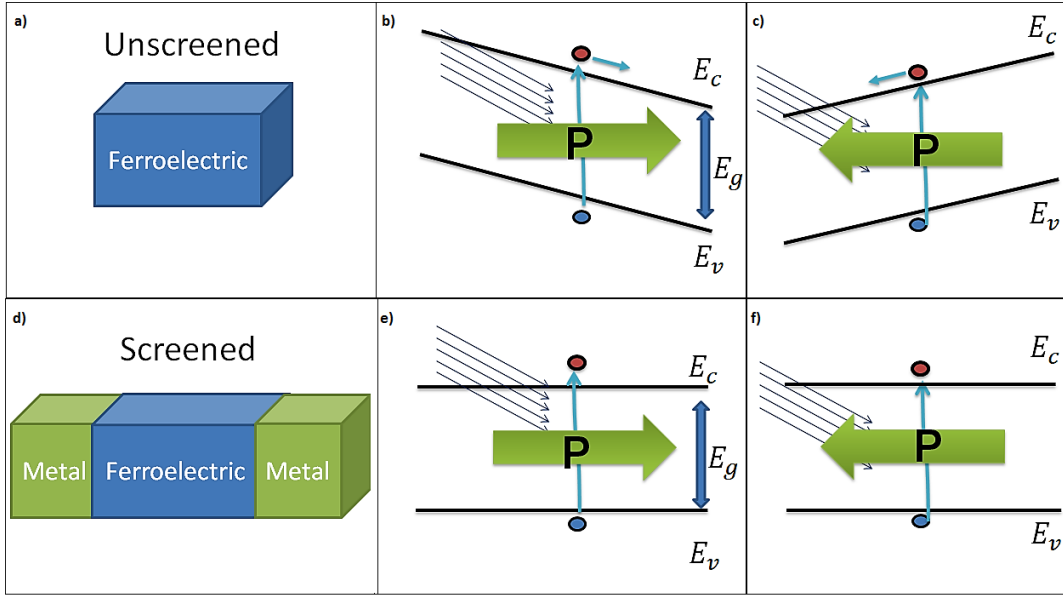
Figure 1. a: Scheme of the sample without electrodes. b, c: Band diagram sketch for each polarization states, it shows the bands tilted due to the field generated by the polarization (not screened). d: Scheme of the sample with electrodes. e, f: Band diagram sketch for each polarization state, it does not show the bands tilted due to $E_{dep} = 0$ (totally screened due to electrodes electrons).

surface barrier. As we can reverse the polarization state we can modify the Schottky barriers[4,12,13].

2.2. Bulk Photovoltaic Effect (BPVE).

There are 20 point symmetry groups which have a not centrosymmetric configuration that show a preferred direction for the induced photo carriers. Ferroelectric materials show this kind of symmetries, which means that for a uniform material under uniform illumination in absence of an applied bias we will find photocurrent. This effect is called bulk photovoltaic effect (BPVE)[14]. BPVE is associated with the violation of balancing principle, there is an asymmetry in the momentum distribution which results in a photocurrent. This violation of the balancing principle is due to inelastic scattering of carriers from asymmetric centres, hopping mechanism between asymmetrically distributed carriers or excitations of impurities centres with an asymmetric potential[15]. Then asymmetry charge generation gives rise to the so-called shift currents without the need to have an electrical gradient. This photovoltage generated by BPVE shows a linear dependence with the distance between electrodes. It is important to mention that in BPVE the photocurrent depends on the crystallographic structure, in particular on the angle between linearly polarized light and structure (or equivalently the material polarization direction.)

2.3. Domain Wall Effect.

Domain wall effect is a mechanism of charge separation and photovoltage generation that takes place at ferroelectric domain walls. This mechanism allows extracting voltages above the bandgap of the ferroelectric material which is one of the main limitations for conventional solar cells. Several articles report that the dependence of the photovoltage with the number of domains, and then with the distance between electrodes, is linear for ferroelectric multi-domain samples while is negligible for single domains samples[16]. Then this effect is related to the domain walls which presents a built-in potential step due to the electric dipoles generated by the bound charges. When the sample is illuminated excitons will be created and separated generating an imbalance of charges near the wall domains giving rise to a net voltage along the sample. Although the role of domain walls on photocurrent is clear, the presented scenario is still under debate by the scientific community [17,18,19]

3. Experimental Description.

$Pt/LuMnO_3/Pt$ samples consist in a $LuMnO_3$ single crystal $(200\mu m)$ sandwiched between Pt-sputtered electrodes. In one side of the crystal, Pt has been deposited through a shadow mask defining square contact pads $50\mu m$ width by RF sputtering.

Ferroelectric measurements were performed using a planar capacitor configuration. The polarization was evaluated by measuring the dynamic P-E hysteresis loops and I-V curves using a TFAnalyzer2000 (aixACCT Systems GmbH) in a range of frequencies between 10Hz and 1KHz at room temperature. The current-voltage (J-V) characteristics of the sample in dark conditions and under illumination was characterized using a Keithley 617 programmable electrometer.

Polarization effect measurements were performed by polling the sample in a given direction with a triangular pulse of 150V applied for 2 s, to saturate it in one polarization state, or measuring the reverse polarization state effect, using an identical pulse in the opposite direction, during the same time (τ_{FE}). After applying the triangular pulse to polarize the sample we wait 10 seconds to start to measure avoiding transient effects. The remnant polarization is determined integrating the current through the measuring circuit. As commonly observed when using ex-situ grown metal electrodes, the response is found to be somehow depending on the particular contact (or pair of contacts) considered. We have tested more than 30 of them and selected the ones in which the effects of ferroelectricity are more representative. Fig. 2 shows the electrical configuration used for these measurements.

Illuminating of the $Pt/LuMnO_3/Pt$ sample has been done with a blue laser of wavelength 405 nm and 200 μm spot feed by a CPX400SA DC power source (AimTTi Co.). We strength here that the used photons (blue; 3.06 eV) are of above-bandgap energy (1.5 eV for $LuMnO_3$ [10]).

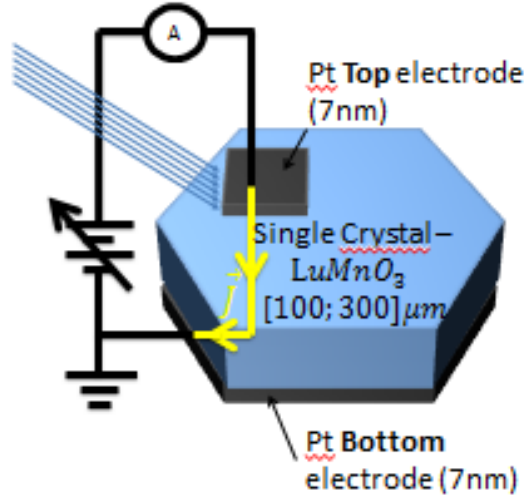Finally to evaluate the dependence of the response with wavelength and with the

Figure 2. Electric contact configuration used to measure.

polarization relative direction of light and material, we use a linear polarize STEC power supply module V 1.0 which allows to control the output power for 4 different wavelengths (405nm; 450nm; 520nm; 638nm) feed by a CPX400SA DC power source (AimTTi Co.). For these measurements, we selected an output density power of $P = 1.5W/cm^2$.

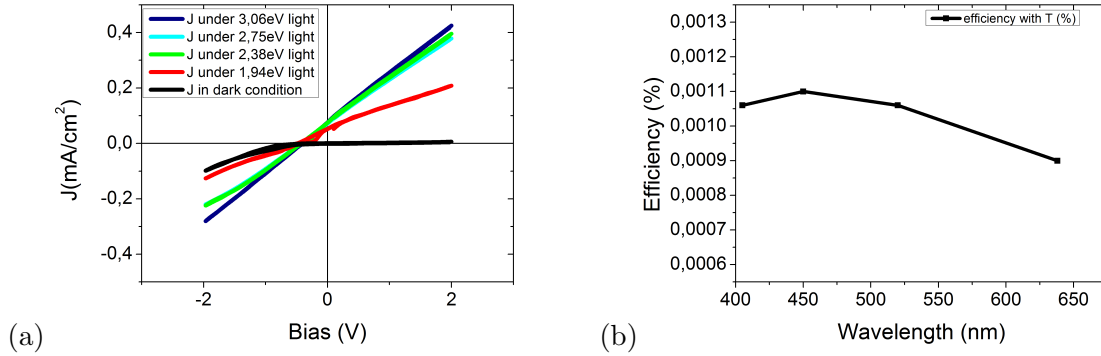## 4. Results and Discussion.

(a)

(b)

Figure 3. a): J-V curves for dark condition and under different energy photons illumination. b): Calculated efficiency for each wavelength.

The results obtained for the photo-response are shown in Fig 3. All of our $Pt/LuMnO_3/Pt$ samples exhibited a one-side diode behaviour in dark conditions as it has been reported for several ferroelectric materials like BFO[20]. As shown in Fig. 3 a) the J-V curve indicated a diode effect with negative forward bias (reverse diode). Under illumination Fig. 3 shows that $Pt/LuMnO_3/Pt$ capacitors response for the 4 illumination wavelength like it was expected because literature fixes experimentally

$Eg \simeq 1.5eV$ by Tauc model[9]. An anomalous behaviour is found for $1.94eV$ photons (red). In principle every wavelength photons have an energy above the bandgap, then each photon should create an electron hole pair that will be drain obtaining the photocurrent, so we should obtain the same photocurrent under different illuminations. As shown in Fig. 3 a) the red photons generate a smaller current, this could be explained due to absorption near E_g is not total.

Another anomalous behaviour is the change from diode to ohmic. It can be explained due to defects. Previous literature reports that $LuMnO_3$ use to show Lu vacancies which result in $Lu_{1-x}MnO_{3-\delta}$[21,22]. Then in dark conditions we have a p type semiconductor that allows to move holes in one direction but not in the other due to Schottky barriers while under illumination the generated electrons can move in both sides giving rise to the ohmic behaviour.

In figure 3 b) we show the calculated efficiencies for each wavelength. Like $LuMnO_3$ shows an ohmic behaviour under illumination its field factor will be low (around 25%). The power density of the laser is controllable and known then the efficiency is defined as $\eta = \frac{V_{oc} \cdot I_{sc} \cdot FF}{Pin}$ where FF is the field factor, J_{sc} is the short circuit current, V_{oc} is the open circuit voltage and P_{in} is the optical power arriving at the electrode, so we are evaluating the rate between the input optical power and the output electrical power. As shown Fig 3 b) the efficiency of the device is around $\eta = 10^{-3}\%$ which is small compared to other materials that have been reported[9,23].

Then we should evaluate which are the possible mechanisms that give rise to this low efficiency. Previous literature is focused in thin film so it could be that this difference is related to the fact that we are studying single crystal response (thick sample). Then the recombination until extract the photocarriers increase giving rise to smaller efficiencies[24,25]. This is inherent to our device so we cannot control it. However, another scenario is that the ferroelectric mechanisms are not taking place in the charge separation. The low efficiency value can find its origin in different reasons, in the next sections we have tried find out them by the analysis of the effects of: ferroelectric polarization sign, angle between ferroelectric and light polarization and domain walls effect.

4.1. Ferroelectric Polarization Effect.

In Fig. 4 P-E and J-V loops are shown, our $LuMnO_3$ sample had a remnant polarization around $10\mu C/cm^{-2}$. The coercive voltages of the device are approximately symmetric with a value around $V_c = 53V$. This symmetry in the loops says that the imprint field is quite small in the sample[26].Knowing the polarization of the sample and the relative permittivity ($\epsilon_r \simeq 22$[27]) we can obtain the value of the depoling field if there is not screening, $E_d \simeq P/\epsilon\epsilon_0 \simeq 49 * 10^2 KV/cm$. This is not the case because is known that the electrodes will contribute charges to screen this field reducing its value. In the right figure we can distinguish the switching current due to the change of polarization state. This current is generated by the screening charges that flows when the polarization
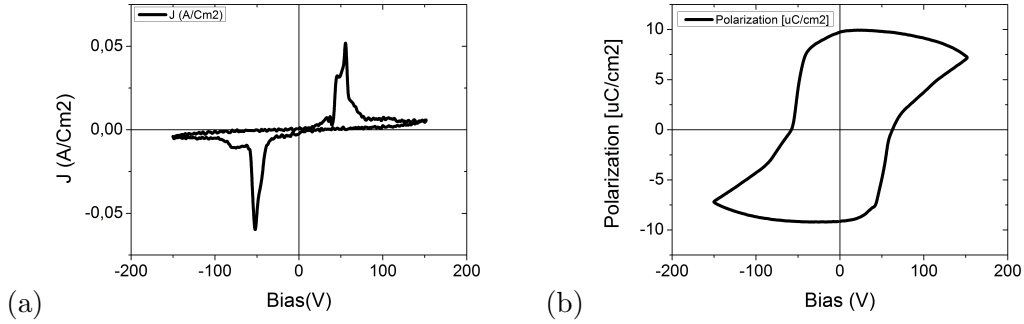
switches due to electrostatic repulsion.

(a)   (b)

Figure 4.   a): Density current-voltage loop of the $LuMnO_3$ capacitor.   b): Polarization-voltage hysteresis loop of the $LuMnO_3$ capacitor.

We used the electrometer applying a bias and recording the generated current for dark conditions and under illumination. We have defined the positive voltage applied to the top electrode and vice versa and the positive sign of the current flowing positive charges from the top electrode to the bottom one as indicated by the arrow in Fig 2.

In order to explore the effect of polarization, we prepoled the sample in both directions allowing to distinguish the response between them. Let's define the polarization states, as it was said in the experimental section we apply the pulse in the top electrode. Applying a positive voltage we obtain a downward polarization while when we apply a negative voltage it generates the upward polarization as can be seen in the Fig.5.
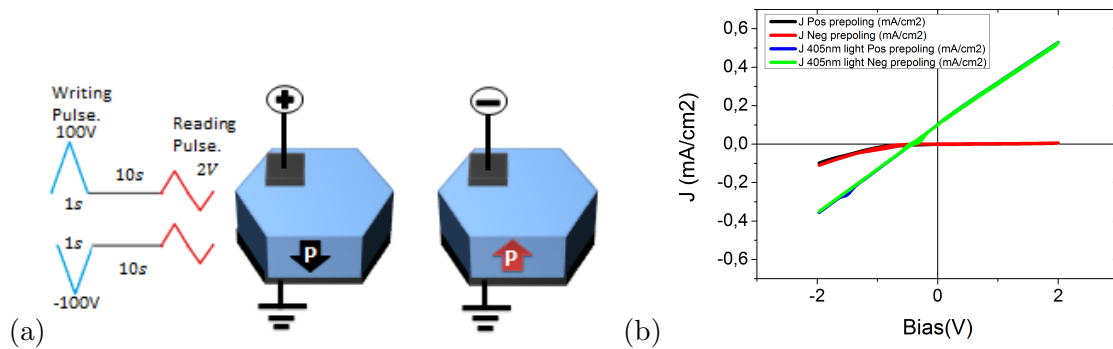

(a)   (b)

Figure 5.   a): Prepoling pulse scheme and electric contact configuration used to measure.   b): J-V curves for dark condition and under illumination for both polarization states.

The J-V curves show that there is not change in the behaviour depending on the polarization state. The photoresponse remains constant independently of the prepoling. Then we conclude that we are in a scenario shown in the Fig 1 (d,e,f) where the depolarization field is totally screened and then it does not take place in the separation of the photocharges. Asymmetric samples were studied obtaining similar results.

4.2. Angle between light and ferroelectric polarization.

Then, we decided to evaluate the dependence of the photoresponse with polarization of light. For this purpose, we used a linear polarized laser as it was said in the experimental section. In order to study this effect, we created a set up with two goniometer that allows to rotate the sample and then, change the relative angle between the material and light polarization (Fig 6 a)). We compare the expected theoretical increase of the photoresponse when the incidence goes to orthonormal with the experimental results. The results are shown in the Fig 6 b).
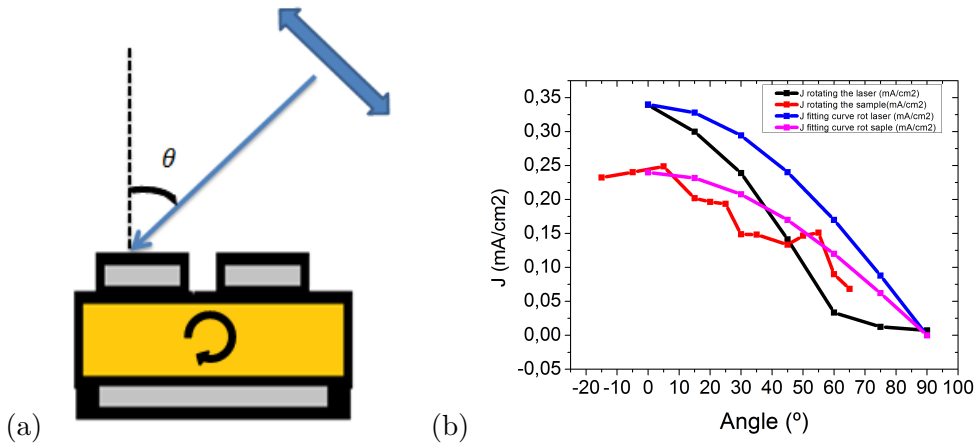

(a)   (b)

Figure 6. a): Scheme movement obtained with the set up. b): J-angle curves under linear polarized laser light. Theoretical expected values and experimental.

It can be seen that there are difference between the theoretical and experimental values, then, it looks that some extra mechanism is taking place. As it was said in the state of the art ferroelectric materials shows a preference direction so this effect seems to be related with the BPVE, although the effect is small.

4.3. Domain Wall Effect.

Finally, we studied the effect of walls domain. In order to evaluate this effect, we generated multiple ferroelectric domains applying pulses with smaller voltages successively, as it can be seen in the Fig 7 a), generating several domains with different polarization orientation. An increase in the photoconductivity was found when we do not saturate the sample with a prepoling pulse as it can be seen in the Fig 7 b).

There is a increase of the photoconductivity ($\simeq 15\%$) when the sample shows more ferroelectric domain.
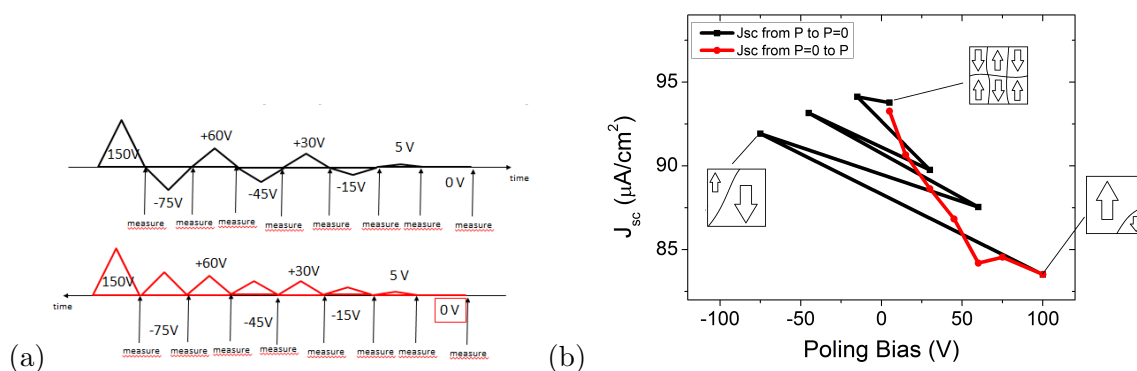
Figure 7. a): Scheme of the applied prepoling pulses. b): J-Prepolig pulse(V) curves under linear polarized laser light.

5. Summary And Conclusions.

In the current report, we focused on the use of ferroelectric small gap material for photovoltaic application. We have demonstrated that $LuMnO_3$ has photoresponse at low light energies giving rise to low efficiencies compared with ferroelectric films of wider bandgap materials independently of the polarization state. We suggested that the low efficiency is because the effect of depolarization field on photocurrent is not present due to the perfect screening of the polarization by electrodes. The effect of the angle between the light and ferroelectric polarization is low and then it is difficult to evaluate. The difficulty to contact with the tips to electrodes made this evaluation harder. The appearance of multi-ferroelectric domains in the sample produces an increase of the photoconductivity in the material due to wall domain effects.

Further studies could be done trying to avoid the perfect screening of the polarization by electrodes. Then the next step to evaluate the influence of depolarization field is depositing a insulate (oxide) layer between the electrodes and $LuMnO_3$. In this way, we will avoid free charges form the electrodes screen perfectly the polarization bound charges giving rise to a depolarization field through the device. We tried to obtain this sample but several technical problems were found in the PLD (Pulsed Laser Deposition) giving not choice to create this scenario.

6. Bibliography

[1] S. De Wolf, et al., *High-efficiency Silicon Heterojunction Solar Cells: A Review* **Vol.2**, pp 7-24, 2012.
[2] M.A. Green, *The path to 25% silicon solar cell efficiency: History of silicon cell evolution.* Progress in Photovoltaic **Vol.17**, pp 183-189, 2009.
[3] T. Butler, et al., *Ferroelectric materials for solar energy conversion: photoferroics revisited* Royal Society of Chemistry **Vol.**, pp 838, 2015.
[4] C. Paillard et al., *Photovoltaics with Ferroelectrics: Current Status and Beyond* Advance Materials. **Vol.28**, pp 5153-5168 , 2009.

[5] K. YAO, ET AL.,*Large photo-induced voltage in a ferroelectric thin film with in-plane polarization.* Appl. Phys. Lett **87**, 212906, 2005.

[6] S.M. SZE *Physics of semiconductor devices.* John Wiley and Sons, New York. **2°ed**, 1981.

[7] D. LEE, ET AL.,*Polarity control of carrier injection at ferroelectric/metal interfaces for electrically switchable diode and photovoltaic effect.* Physical Review B **Vol.84**, 125305, 2011.

[8] F. WANG, ET AL., *Band gap engineering strategy via polarization rotation in perovskite ferroelectric.* Appl. Phys. Lett **Vol.104**, 152903, 2014.

[9] H. HANS, ET AL., *Switchable photovoltaic effects in hexagonal manganite thin films having narrow band gaps.* Chem. Mater. **Vol.27**, pp. 25-32, 2014.

[10] W. SHOCKLEY and J. QUEISSER, *Detailed balance limit of efficiency of p-n junction solar cells.* Appl. Phys. Lett **Vol.32**, pp. 510-519, 1961.

[11] L. PINTILIE and M. ALEXE *Metal-ferroelectric-metal heterostructures with Schottky contacts. Influence of the ferroelectric properties* Appl. Phys. Lett **Vol.98**, pp. 103-124, 2005.

[12] G.L.YUAN and J. WANG *Evidences for the depletion region induced by the polarization of ferroelectric semiconductors* Appl. Phys. Lett. **Vol.95**, issue 25, 2009.

[13] L. FANG ET AL., *Switchable photovoltaic response from polarization modulated interfaces in BiFeO3 thin films* Appl. Phys. Lett. **Vol.104**, issue 14, 2014.

[14] R. VON BALTZ, and W. KRAUT *Theory of the bulk photovoltaic effect in pure crystals.* Physics Review B. **Vol.23**, issue 10, 1981.

[15] V.M FRIDKIN *Bulk Photovoltaic Effect in Noncentrosymmetric Crystals* Crystallography Reports **Vol.46**, pp. 654-658, 2001.

[16] S.Y. YANG, ET AL., *Above-bandgap voltages from ferroelectric photovoltaic devices.* Nature Nanotechnology **Vol.5**, pp. 143-147, 2010.

[17] A. BHATNAGAR ET AL., *Role of domain walls in the abnormal photovoltaic effect in BiFeO3.* Nature Communications **Vol.4**, art. n. 2835, 2013.

[18] M. ALEXE ET AL., *Tip-enhancement photovoltaic effects in bismuth ferrite* Nature Communications **Vol.2**, art. n. 256, 2011.

[19] M. ALEXE ET AL., *Local mapping of generation and recombination lifetime in $BiFeO_3$ single crystal by scanning probe photoinduced transient spectroscopy* Nano Lett. **Vol.12**, pp. 2193-2198, 2012

[20] T. CHOI, ET AL., *Switchable ferroelectric diode and photovoltaic effect in $BiFeO_3$.* Science **Vol.324**, pp. 63-66, 2009.

[21] N. IMAMURA ET AL., *Hole doping into the metastable $LuMnO_3$ perovskite.* Solid State Communication **Vol.140**, pp. 386-390, 2006.

[22] H. CHIBA ET AL., *Magnetic and Electrical Properties of $Bi_{1-x}Sr_xMnO_3$: Hole-Doping Effect on Ferromagnetic Perovskite $BiMnO_3$* Journal Solid State Chemistry **Vol.132**, pp. 139-143, 1997.

[23] K. SHARMAN and A. SINGH, *Advance in photovoltaic behavior of ferroelectric $BiFeO_3$.* Journal of Nanoscience and Technology **Vol.2**, pp 85-90, 2016.

[24] M.STOLTERFOHT ET AL., *Photocarrier drift distance in organic solar cells and photodetectors* Scientific Reports **Vol.5**, art. n. 9949, 2015.

[25] M. QUIN ET AL., *Thickness effects on photoinduced current in ferroelectric thin films* Journal of applied physics. **Vol.101**, issue 1 , 2007.

[26] F. LIU., *Selecting Steady and Transient Photocurrent Response in BaTiO3 Films.* Advanced electronic materials **Vol.1**, issue 9, 2015.

[27] A. GHOSH ET AL., *A Raman study of multiferroic $LuMnO_3$.* Solid State Science **Vol.11**, pp. 1639-1642, 2009.